STATISTICS, OPTIMIZATION AND INFORMATION COMPUTING
Stat., Optim. Inf. Comput., Vol. **x**, Month 202x, pp 0–23.
Published online in International Academic Press (www.IAPress.org)

Fuzzy Volterra Integral Equation Approximate Solution via Optimal Homotopy Asymptotic Methods

Alzubi Muath Talal Mahmoud [1], Farah Aini Abdullah [1], Ali Fareed Jameel [2], Adila Aida Azahar [1,*]

[1] *School of Mathematical Sciences, Universiti Sains Malaysia, 11800 USM, Penang, Malaysia*
[2] *Faculty of Education and Arts, Sohar University, Sohar, Oman*

Abstract The field of fuzzy integral equations (FIEs) is significant for modeling complex, time-delayed, and uncertain physical phenomena. Nevertheless, the majority of current solutions for FIEs encounter considerable challenges, such as the inability to manage intricate fuzzy functions, stringent assumptions regarding the forms of fuzzy operations utilized, and numerical instability in extremely nonlinear issues. Moreover, the capability of traditional methods in producing precise or reliable outcomes for practical applications is limited, and if they can, will incur substantial computing expenses. These challenges underscore the demand for more effective and efficient methodologies. This study aims to address the demand by developing two approximate analytical techniques to solve the FIEs namely optimal homotopy asymptotic method (OHAM) and the multistage optimal homotopy asymptotic method (MOHAM). A novel iteration of fuzzy OHAM and MOHAM is introduced by integrating the fundamental concepts of these methodologies with fuzzy set theory and optimization techniques. Then, OHAM and MOHAM are further formulated to solve the second-kind linear Volterra fuzzy integral equations (VFIEs). These methods are named fuzzy Volterra optimal homotopy asymptotic method (FV-OHAM) and fuzzy Volterra multistage optimal homotopy asymptotic method (FV-MOHAM), respectively. From two linear examples, FV-MOHAM and FV-OHAM generated significantly more accurate results than other existing methods. A thorough assessment is performed to evaluate their effectiveness and practical use, potentially aiding in solving complex problems across several scientific and engineering fields.

Keywords Fuzzy Integral Equations (FIEs), Fuzzy Volterra Integral Equations (FVIEs), Optimal Homotopy Asymptotic Method (OHAM), Multistage Optimal Homotopy Asymptotic Method (MOHAM)

DOI: 10.19139/soic-2302

1. Introduction

Integral equations encompass an unknown function within a definite integral [1]. These equations are closely related to differential equations. They are used to investigate the properties of equations which can further be applied to formulate both approximate and numerical solutions [2]. Integral equations provide a flexible approach for problem-solving by converting problems to integral equations or vice versa [3]. Ordinary and partial differential equations are frequently employed to tackle initial and boundary value problems [4]. Furthermore, integral equations are essential in the theoretical and numerical examination of differential equations, with their foundations based on elementary analysis. The methodology of integral equations is utilized in solving thermal engineering problems, such as radiative heat transfer and heat conduction [5]. Integral equations arise in several scientific and technical contexts and can be derived from both starting and boundary value issues. In this study, we are interested in a class of integral equations called Volterra integral equations. These equations describe systems involving

*Correspondence to: Adila Aida Azahar (Email: adilaazahar@usm.my). School of Mathematical Sciences, Universiti Sains Malaysia, 11800 USM, Penang, Malaysia.

ISSN 2310-5070 (online) ISSN 2311-004X (print)

memory effects or temporal evolution, such as population dynamics and biological reactions [6]. Recent studies have proposed algorithms for solving linear and non-linear Volterra integro-differential equations effectively [7].

Fuzzy integral equations (FIEs) are a significant component of fuzzy analytic theory, with extensive applications in physics, mechanics, medicine, and control engineering [8]. Numerous approaches have been formulated to solve these problems. These approaches usually convert fuzzy integrals into parametric Riemann integrals [9], enabling the application of uniform approximation algorithms. This development has facilitated the progress of soft computing systems designed to address our equations of interest, the second-kind fuzzy Volterra integral equations (FVIEs) [10]. Some existing numerical methods to solve these equations are as follows: a numerical approach utilizing the residual minimizing methodology [11], a sixth-order Runge-Kutta method [12], an iterative numerical method integrating successive approximations using a combination of mixed trapezoidal and midpoint criteria [13], and an iterative technique using fuzzy Bernstein polynomials [14]. On the other hand, analytical approximation techniques such as the Adomian decomposition method, variational iteration method, and homotopy analysis method (HAM) are also extensively utilized to approximate solutions to second-kind FVIEs [15]. HAM particularly shines in regulating the convergence behaviour of solution series by integrating an auxiliary parameter, facilitating swift and dependable convergence [16, 17]. The adaptability of HAM and its incorporation with various approximation methods render it an effective instrument for solving FIEs [18].

The Optimal Homotopy Asymptotic Method (OHAM), an improved version of HAM, is a powerful approximation technique widely employed in engineering and scientific disciplines. OHAM has been used in solving elastic stress issues in spinning discs [19], generating analytical solutions for nonlinear oscillators [20], and tackling time-fractional Navier-Stokes equations in conjunction with the Laplace transform [21], to name a few. In addition, the multistage optimum homotopy asymptotic method (MOHAM) enhances the usefulness of the OHAM, especially in addressing fractional optimal control problems [22]. Like OHAM, MOHAM has also been successfully employed in solving initial-value problems [23]. Notwithstanding these developments, considerable hurdles persist in implementing OHAM and MOHAM in large-scale or computationally intricate applications. Current research frequently concentrates on certain issue categories, such as FVIEs, without adequately assessing the scalability and processing efficiency of the approaches employed. This deficiency obstructs their further use in actual contexts, especially for extensive FIEs.

This study introduces a rigorous analysis of the fuzzy Volterra optimal homotopy asymptotic method (FV-OHAM) and the fuzzy Volterra multistage optimal homotopy asymptotic approach (FV-MOHAM). These methodologies expand the fundamental tenets of OHAM and MOHAM into the fuzzy environment by integrating sophisticated fuzzy set theory notions and optimization-oriented homotopy techniques. This synthesis improves the convergence characteristics and numerical results of the original approaches, rectifying the previously discussed deficiencies in scalability and computational efficiency for extensive FIEs. This paper illustrates, via extensive numerical investigations and comparative analysis, that FV-OHAM and FV-MOHAM can generate better solutions compared with other existing method such as HAM and the iterative fuzzy Bernstein polynomials method (IFBPM) for solving linear FVIEs. Additionally, a theoretical framework is established to guarantee the convergence of solutions utilizing these methods, while improving computational efficiency in large-scale applications. The developments in this work are seeking to facilitate their widespread implementation by addressing practical difficulties across several scientific and technical disciplines.

The choice of FV-OHAM and FV-MOHAM methodologies in this study is strategically motivated by several key factors. First, these methods provide convergence control through their auxiliary parameters [24], determined by minimizing the square residual error [25]. These parameters are used to adjust and control the convergence region and rate of the series solution [26]. The OHAM method is distinguished by providing multiple convergence control parameters, allowing greater flexibility in adjusting the convergence region [27], unlike traditional perturbation techniques. Second, they demonstrate remarkable accuracy in handling linear FVIEs, achieving significantly smaller errors compared to existing methods such as HAM and IFBPM. Third, these approaches maintain consistent performance across different parameter values while preserving fuzzy properties throughout. Fourth, high accuracy is achieved with lower-order approximations, resulting in improved computational efficiency. This combination of theoretical elegance, computational efficiency, and practical applicability makes these methods particularly suitable for solving FVIEs while addressing the current limitations.

2. Preliminaries

In this section, we review the fundamental notations of fuzzy set theory to be used throughout this paper.

Definition 2.1
A fuzzy number u is a pair $(\underline{u}, \overline{u})$ of functions $\underline{u}(r), \overline{u}(r)$; $0 \leq r \leq 1$ which satisfies the following requirements:

i. $\underline{u}(r)$ is a bounded left-continuous non-decreasing function over $[0, 1]$,

ii. $\overline{u}(r)$ is a bounded left-continuous non-increasing function over $[0, 1]$,

iii. $\underline{u}(r) \leq \overline{u}(r), 0 \leq r \leq 1$.

A crisp number α is simply represented by $\underline{u}(r) = \overline{u}(r) = \alpha, 0 \leq r \leq 1$. The set of all fuzzy numbers is denoted by E^1 [28, 29].

For arbitrary fuzzy numbers $u = (\underline{u}, \overline{u}), v = (\underline{v}, \overline{v})$ and an arbitrary crisp number k, we define the fuzzy addition and the scalar multiplication as follows:

i. $(\underline{u+v})(r) = (\underline{u}(r) + \underline{v}(r))$,

ii. $(\overline{u+v})(r) = (\overline{u}(r) + \overline{v}(r))$,

iii. $(\underline{ku})(r) = k\underline{u}(r), (\overline{ku})(r) = k\overline{u}(r), k \geq 0$,

iv. $(\underline{ku})(r) = k\overline{u}(r), (\overline{ku})(r) = k\underline{u}(r), k < 0$.

3. Analysis of Fuzzy Volterra Integral Equations

An integral equation is a foundational concept in mathematics and physics, expressing a relationship whereby an unknown function $\varphi(x)$ appears inside an integral over a specified interval $[a, b]$. Mathematically, it is represented as:

$$\varphi(x) = \int_a^b k(x,t)\,\varphi(x)\,dt, \tag{1}$$

where $k(x,t)$ is the kernel function that governs the interaction between the values of $\varphi(x)$ and $\varphi(t)$ across the interval $[a, b]$. A Fredholm integral equation of the second kind extends this framework by incorporating a known function $f(x)$ and a constant parameter $\lambda \in R$:

$$\varphi(x) = \lambda \int_a^b k(x,t)\,\varphi(t)\,dt + f(x). \tag{2}$$

Equation (2) encapsulates integral transformations where $\varphi(x)$ depends on its integral concerning $\varphi(t)$ weighted by $k(x,t)$ coupled with an external forcing term $f(x)$. In contrast, a VIE of the second kind alters the integration limits to include x as the upper limit:

$$\varphi(x) = \lambda \int_a^x k(x,t)\,dt\,\varphi(t) + f(x). \tag{3}$$

This type of equation often models systems exhibiting memory effects or time-dependent behaviors, where the integral reflects the cumulative influence of $\varphi(t)$ up to x. Such integral equations are indispensable in analyzing dynamic systems in physics, engineering, and biology, offering powerful analytical tools to study phenomena ranging from wave propagation and diffusion to population dynamics and biochemical kinetics. FIEs innovate beyond classical forms by integrating fuzzy sets and logic, accommodating uncertainties and vague boundaries in real-world data. They provide a robust framework for modeling complex systems, capturing the nuanced and

imprecise nature of real-world phenomena. This extension expands the use of integral equations to handle a broader range of problems with uncertain or ambiguous information.

The second kind of fuzzy Volterra equation is defined as follows:

$$\tilde{v}(s) = \tilde{f}(s) + \tilde{\lambda} \int_a^s \tilde{k}(s,t,\tilde{v}(s)\,dt, \tag{4}$$

where λ is the fuzzy parameter [30], $\tilde{k}$ represents an arbitrary function referred to as the kernel of the integral equation (1) defined over square $G : [a,b] \times [a,b]$, $\tilde{k} = 0$, $a \leq s,t \leq b$, $s > t$, and $\tilde{f}(s)$ is a given fuzzy function of $t \in [a,b]$ with $\tilde{v}(s)$ being the unknown fuzzy function to be determined where $\tilde{f}(s)$ and $\tilde{k}$ be for crisp variable s. Using the defuzzification properties and r-cut set of $\tilde{v}(s)$, we have

$$\tilde{v}(s,r) = \tilde{f}(s,r) + \tilde{\lambda}(r) \int_a^s k\left(s,t,\tilde{v}(t,r),r\right)\,ds, \tag{5}$$

such that

$$\begin{cases} \tilde{v}(s) = \tilde{v}(s;r) = \left[\underline{v}(s;r),\, \overline{v}(s;r)\right], \\ \tilde{k}(s,\tilde{v}(s)) = \tilde{k}(s,\tilde{v}(s;r);r) = \left[\underline{k}(s,\tilde{v}(s;r);r), \overline{k}(s,\tilde{v}(s;r);r)\right], \\ \tilde{\lambda} = \tilde{\lambda}(r) = \left[\underline{\lambda}(r), \overline{\lambda}(r)\right], \\ \tilde{f}(s) = \tilde{f}(s;r) = \left[\underline{f}(s;r), \overline{f}(s;r)\right], \end{cases} \tag{6}$$

with $0 \leq s \leq 1$.

By using equation (3), the solution for equation (1) can be obtained by solving the following two integral equations:

$$\begin{cases} \underline{x}(t;r) = \underline{f}(t;r) + \underline{\lambda}(r) \int_a^x \underline{k}\left(t,s,\underline{v}(s;r)\right) ds, \\ \overline{x}(t;r) = \overline{f}(t;r) + \overline{\lambda}(r) \int_a^x \overline{k}\left(t,s,\overline{v}(s;r)\right) ds. \end{cases} \tag{7}$$

The fuzzy function $\tilde{k}$ can be written as follows:

$$\begin{cases} \underline{k}(s,\tilde{v}(s;r);r) = \mathcal{F}\left[s,\underline{v},\overline{v}\right]_r, \\ \overline{k}(s,\tilde{v}(s;r);r) = \mathcal{G}\left[s,\underline{v},\overline{v}\right]_r. \end{cases} \tag{8}$$

By using the extension fuzzy principle:

$$\begin{cases} \mathcal{F}\left[s,\underline{v},\overline{v}\right]_r = min\left\{\tilde{k}\left(s,\tilde{\mu}(r)\right) : \tilde{\mu}(r) \in \tilde{v}(s;r)\right\} \\ \mathcal{G}\left[s,\underline{v},\overline{v}\right]_r = max\left\{\tilde{k}\left(s,\tilde{\mu}(r)\right) : \tilde{\mu}(r) \in \tilde{v}(s;r)\right\} \end{cases} \tag{9}$$

equation (8) becomes

$$\begin{cases} \underline{k}(s,\tilde{v}(s;r);r) = \mathcal{F}\left(s,\underline{v}(s;r),\overline{v}(s;r)\right) = \mathcal{F}\left(s,\tilde{v}(s;r)\right), \\ \overline{k}(s,\tilde{v}(s;r);r) = \mathcal{G}\left(s,\underline{v}(s;r),\overline{v}(s;r)\right) = \mathcal{G}\left(s,\tilde{v}(s;r)\right). \end{cases} \tag{10}$$

This procedure is called the defuzzification technique [31]. The necessary conditions for the existence of a unique solution to equation (3) are presented and demonstrated by Kaleva [29].

4. Formulation of Fuzzy Optimal Homotopy Asymptotic Method

This section discusses the basic idea of fuzzy OHAM [31]. Its formulation, $\varphi(s;q;r) : [s_0,S] \times [0,1] \to \mathbb{R}$, satisfies the following:

$$(1-q)\left[\tilde{\mathcal{L}}\left(\tilde{\varphi}(s;q;r)\right) - \tilde{f}(s;r)\right] = \tilde{\mathcal{H}}(q;r)\left[\tilde{\mathcal{L}}\left(\tilde{\varphi}(s;q;r)\right) - \tilde{k}\left(s,\tilde{v}(s;r)\right) - \tilde{f}(s;r)\right], \tag{11}$$

where $q \in [0,1]$ is an embedding parameter. For $q \neq 0$, the auxiliary function $\tilde{\mathcal{H}}(q;r) = [\underline{\mathcal{H}}(q;r), \overline{\mathcal{H}}(q;r)]$ and $\tilde{\varphi}(s;q;r)$ is the unknown fuzzy function. For $q = 0$, $\tilde{\mathcal{L}} = [\underline{\mathcal{L}}, \overline{\mathcal{L}}] = [\underline{\varphi}(s;q;r), \overline{\varphi}(s;q;r]$ and $\tilde{\varphi}(s;0;r) = \tilde{v}_0(s)$, which is the initial guess. For $q = 1$, $\tilde{\varphi}(s;1;r) = \tilde{v}(s)$, which is the exact solution. The dynamic of fuzzy OHAM is given by:

$$\underline{\mathcal{L}}(\underline{v}(s;r) - \mathcal{F}\left(s, \tilde{v}(s;r)\right) - \underline{f}(s;r) = 0, \tag{12}$$

$$\overline{\mathcal{L}}(\overline{v}(s;r) - \mathcal{G}\left(s, \tilde{v}(s;r)\right) - \overline{f}(s;r) = 0, \tag{13}$$

$$(1-q)\left[\underline{\mathcal{L}}(\underline{\varphi}(s;q;r)) - \underline{f}(s;r)\right] = \underline{\mathcal{H}}(q;r)\left[\underline{\mathcal{L}}(\underline{\varphi}(s;q;r)) - \underline{\mathcal{F}}(s, \tilde{v}(s;r)) - \underline{f}(s;r)\right], \tag{14}$$

$$(1-q)\left[\overline{\mathcal{L}}(\overline{\varphi}(s;q;r)) - \overline{f}(s;r)\right] = \overline{\mathcal{H}}(q;r)\left[\overline{\mathcal{L}}(\overline{\varphi}(s;q;r)) - \mathcal{G}(s, \tilde{v}(s;r)) - \overline{f}(s;r)\right], \tag{15}$$

where the lower and upper fuzzy linear operators are associated with the lower and upper auxiliary fuzzy functions. The terms $\underline{\varphi}(s;q;r)$ and $\overline{\varphi}(s;q;r)$ are the lower and upper unknown fuzzy functions, respectively. When $q = 0$ and $q = 1$, we have equation (16) and (17), respectively.

$$\underline{\varphi}(s;0;r) = \underline{v}_0(s;r), \qquad \underline{\varphi}(s;1;r) = \underline{v}(s;r). \tag{16}$$

$$\overline{\varphi}(s;0;r) = \overline{v}_0(s;r), \qquad \overline{\varphi}(s;1;r) = \overline{v}(s;r). \tag{17}$$

Therefore, when q increases from 0 to 1, the solution $\tilde{\varphi}(s;q;r)$ varies from $\overline{v}_0(s;r)$ to the exact solution. When $q = 0$, the lower and upper bounds of zeroth order are:

$$\underline{\mathcal{L}}(\underline{\varphi}(s;0;r)) = \underline{f}(s;r), \qquad \overline{\mathcal{L}}(\overline{\varphi}(s;0;r)) = \overline{f}(s;r). \tag{18}$$

The auxiliary function $\tilde{\mathcal{H}}(q;r)$ for equations (14) and (15) are:

$$\begin{cases} \underline{\mathcal{H}}(q;r) = \sum_{j=1}^{\infty} \underline{\mathcal{C}}_j(r) q^j = \underline{\mathcal{C}}_1(r) q^1 + \underline{\mathcal{C}}_2(r) q^2 + \cdots, \\ \overline{\mathcal{H}}(q;r) = \sum_{j=1}^{\infty} \overline{\mathcal{C}}_j(r) q^j = \overline{\mathcal{C}}_1(r) q^1 + \overline{\mathcal{C}}_2(r) q^2 + \cdots, \end{cases} \tag{19}$$

where $\tilde{\mathcal{C}}_1(r) = \left[\overline{\mathcal{C}}_1(r), \overline{\mathcal{C}}_2(r)\right]$, $\tilde{\mathcal{C}}_2(r) = \left[\underline{\mathcal{C}}_2(r), \overline{(\mathcal{C}}_2(r)\right], \ldots$ are the auxiliary convergence constants. Expanding the solution $\tilde{\varphi}(s;q;r)$ about q by Taylor's series yields the series approximate solution via fuzzy OHAM:

$$\begin{cases} \underline{\varphi}\left(s;q;\underline{\mathcal{C}}_j(r);r\right) = \underline{v}_0(s;r) + \sum_{j=1}^{\infty} \underline{v}_j\left(s;\underline{\mathcal{C}}_j(r);r\right) q^j. \\ \overline{\varphi}\left(s;q;\overline{\mathcal{C}}_j(r);r\right) = \overline{v}_0(s;r) + \sum_{j=1}^{\infty} \overline{v}_j\left(s;\overline{\mathcal{C}}_j(r);r\right) q^j. \end{cases} \tag{20}$$

Substituting equations (19) and (20) into equations (14) and (15), and collecting the coefficient of like powers of q to find the lower and upper bounds lead to a system of linear equations. The system for the zeroth order is given in Equation (14). The system for the first-order are obtained as follows:

$$\begin{cases} \underline{\mathcal{L}}\left(\underline{v}_1(s;r)\right) - \underline{\mathcal{L}}\left(\underline{v}_0(s;r)\right) + \underline{f}(s) = \underline{\mathcal{C}}_1(r)\left(\underline{\mathcal{L}}(\underline{v}_0(s;r)) - \underline{\lambda}(r)\int_a^t \mathcal{F}_0\left(\underline{v}_0(s;r)\right) ds - \underline{f}(s;r)\right), \\ \overline{\mathcal{L}}\left(\overline{v}_1(s;r)\right) - \overline{\mathcal{L}}\left(\overline{v}_0(s;r)\right) + \overline{f}(s) = \overline{\mathcal{C}}_1(r)\left(\overline{\mathcal{L}}(\overline{v}_0(s;r)) - \overline{\lambda}(r)\int_a^t \mathcal{F}_0\left(\overline{v}_0(s;r)\right) ds - \overline{f}(s;r)\right). \end{cases} \tag{21}$$

The problem of second-order is defined as follows:

$$\begin{cases} \underline{\mathcal{L}}(\underline{v}_2(s;r)) - \underline{\mathcal{L}}(\underline{v}_1(s;r)) = \underline{\mathcal{C}}_1(r)\underline{\mathcal{L}}(\underline{v}_1(s;r)) - \underline{\mathcal{C}}_1(r)\underline{\lambda}(r)\int_a^t \mathcal{F}_1(\underline{v}_0(s;r))ds \\ -\underline{\mathcal{C}}_2(r)\underline{\lambda}(r)\int_a^t \mathcal{F}_0(\underline{v}_0(s;r))ds - \underline{f}(s;r), \\ \overline{\mathcal{L}}(\overline{v}_2(s;r)) - \overline{\mathcal{L}}(\overline{v}_1(s;r)) = \overline{\mathcal{C}}_1(r)\overline{\mathcal{L}}(\overline{v}_1(s;r)) - \overline{\mathcal{C}}_1(r)\overline{\lambda}(r)\int_a^t \mathcal{F}_1(\overline{v}_0(s;r))ds \\ -\overline{\mathcal{C}}_2(r)\overline{\lambda}(r)\int_a^t \mathcal{G}_0(\overline{v}_0(s;r))ds - \overline{f}(s;r). \end{cases} \tag{22}$$

The general form of the governing problem via fuzzy OHAM of k^{th} order:

$$\begin{cases} \underline{\mathcal{L}}(\underline{v}_k(s;r)) - \underline{\mathcal{L}}(\underline{v}_{k-1}(s;r)) = \underline{\mathcal{C}}_1(r)\underline{\mathcal{L}}(\underline{v}_{k-1}(s;r)) + \sum_{i=2}^{k-1}\underline{\mathcal{C}}_i(r)\left[\underline{\mathcal{L}}(\underline{v}_{k-i}(s;r))\right. \\ -\underline{\lambda}(r)\sum_{i=1}^{k}\int_a^s \underline{\mathcal{C}}_i(r)\mathcal{F}_{k-i}(\underline{v}_0(s;r),\underline{v}_1(s;r),\ldots,\underline{v}_i(s;r)) - \underline{f}(s;r), \\ \overline{\mathcal{L}}(\overline{v}_k(s;r)) - \overline{\mathcal{L}}(\overline{v}_{k-1}(s;r)) = \overline{\mathcal{C}}_1(r)\overline{\mathcal{L}}(\overline{v}_{k-1}(s;r)) + \sum_{i=2}^{k-1}\overline{\mathcal{C}}_i(r)\left[\overline{\mathcal{L}}(\underline{v}_{k-i}(s;r))\right. \\ -\overline{\lambda}(r)\sum_{i=1}^{k}\int_a^s \overline{\mathcal{C}}_i(r)\mathcal{G}_{k-i}(\overline{v}_0(s;r),\overline{v}_1(s;r),\ldots,\overline{v}_i(s;r)) - \overline{f}(s;r), \end{cases} \tag{23}$$

where $\mathcal{F}_{k-i}(\tilde{v}_0(s;r),\tilde{v}_1(s;r),\ldots,\tilde{v}_i(s;r))$ and $\mathcal{G}_{k-i}(\tilde{v}_0(s;r),\tilde{v}_1(s;r),\ldots,\tilde{v}_i(s;r))$ are the coefficients of the lower and upper bound of q^k, respectively. Dependent on parameter $\mathcal{C}_1(r)$, $\mathcal{C}_2(r)$, $\ldots,\mathcal{C}_k(r)$, at $q=1$ we have:

$$\begin{cases} \underline{v}(s,\underline{\mathcal{C}}_1(r),\underline{\mathcal{C}}_2(r),\ldots;r) = \underline{v}_0(s;r) + \sum_{i=1}^{\infty}\underline{v}_i(s,\underline{\mathcal{C}}_1(r),\underline{\mathcal{C}}_2(r),\ldots;r), \\ \overline{v}(s,\overline{\mathcal{C}}_1(r),\overline{\mathcal{C}}_2(r),\ldots;r) = \overline{v}_0(s;r) + \sum_{i=1}^{\infty}\overline{v}_i(s,\overline{\mathcal{C}}_1(r),\overline{\mathcal{C}}_2(r),\ldots;r). \end{cases} \tag{24}$$

Approximating the series solution up to the kth term, equation (24) becomes:

$$\begin{cases} \underline{v}_*(s,\underline{\mathcal{C}}_1(r),\underline{\mathcal{C}}_2(r),\ldots,\underline{\mathcal{C}}_k(r);r) = \underline{v}_0(s;r) + \sum_{i=1}^{k}\underline{v}_i\left(s,\underline{\mathcal{C}}_1(r),\underline{\mathcal{C}}_2(r),\ldots,\underline{\mathcal{C}}_i(r);r\right), \\ \overline{v}_*(s,\overline{\mathcal{C}}_1(r),\overline{\mathcal{C}}_2(r),\ldots,\overline{\mathcal{C}}_k(r);r) = \overline{v}_0(s;r) + \sum_{i=1}^{k}\overline{v}_i\left(s,\overline{\mathcal{C}}_1(r),\overline{\mathcal{C}}_2(r),\ldots,\overline{\mathcal{C}}_i(r);r\right). \end{cases} \tag{25}$$

5. Formulation of Fuzzy Volterra Optimal Homotopy Asymptotic Method (FV-OHAM).

This section modifies the formulation of OHAM in Section 4 to solve FVIEs. The formulation of FV-OHAM $\varphi(s;q;r):[s_0,S]\times[0,1]\to\mathbb{R}$ satisfies the following [31]-[32]:

$$(1-q)\left[\tilde{\mathcal{L}}\left(\tilde{\varphi}(s;q;r)\right) - \tilde{f}(s;r)\right] = \tilde{\mathcal{H}}(q;r)\left[\tilde{\mathcal{L}}\left(\tilde{\varphi}(s;q;r)\right) - \tilde{k}(s,\tilde{v}(s;r)) - \tilde{f}(s;r)\right], \tag{26}$$

where $q \in [0,1]$ is an embedding parameter. For $q \neq 0$, the auxiliary function $\tilde{\mathcal{H}}(q;r) = \left[\underline{\mathcal{H}}(q;r), \overline{\mathcal{H}}(q;r)\right]$ and $\tilde{\varphi}(s;q;r)$ is the unknown fuzzy function. For $q = 0$, $\tilde{\mathcal{L}} = \left[\underline{\mathcal{L}}, \overline{\mathcal{L}}\right] = \left[\underline{\varphi}(s;q;r), \overline{\varphi}(s;q;r)\right]$ and $\tilde{\varphi}(s;0;r) = \tilde{v}_0(s)$ which is the initial guess. For $q = 1$, $\tilde{\varphi}(s;1;r) = \tilde{v}(s)$, which is the exact solution. The dynamic of FV-OHAM for solving FVIEs is given by:

$$\begin{cases} \underline{\mathcal{L}}(\underline{v}(s;r)) - \mathcal{F}(s,\tilde{v}(s;r)) - \underline{f}(s;r) = 0, \\ \overline{\mathcal{L}}(\overline{v}(s;r)) - \mathcal{G}(s,\tilde{v}(s;r)) - \overline{f}(s;r) = 0, \\ (1-q)[\underline{\mathcal{L}}(\underline{\varphi}(s;q;r)) - \underline{f}(s;r)] = \underline{\mathcal{H}}(q;r)[\underline{\mathcal{L}}(\underline{\varphi}(s;q;r)) - \mathcal{F}(s,\tilde{v}(s;r)) - \underline{f}(s;r)], \\ (1-q)[\overline{\mathcal{L}}(\overline{\varphi}(s;q;r)) - \overline{f}(s;r)] = \overline{\mathcal{H}}(q;r)[\overline{\mathcal{L}}(\overline{\varphi}(s;q;r)) - \mathcal{G}(s,\tilde{v}(s;r)) - \overline{f}(s;r)], \end{cases} \tag{27}$$

where the lower and upper fuzzy linear operators are associated with the lower and upper auxiliary fuzzy functions. The terms $\left[\underline{\varphi}(s;q;r), \overline{\varphi}(s;q;r)\right]$ are the lower and upper unknown fuzzy functions, respectively. When $q = 0$ and $q = 1$, we have equation (28).

$$\begin{aligned} \underline{\varphi}(s;0;r) &= \underline{v}_0(s;r), \quad & \underline{\varphi}(s;1;r) &= \underline{v}(s;r). \\ \overline{\varphi}(s;0;r) &= \overline{v}_0(s;r), \quad & \overline{\varphi}(s;1;r) &= \overline{v}(s;r). \end{aligned} \tag{28}$$

Therefore, when q increases from 0 to 1, the solution $\tilde{\varphi}(s;q;r)$ varies from $\tilde{v}_0(s;r)$ to the exact solution. When $q = 0$, the lower and upper bounds of zeroth order are:

$$\underline{\mathcal{L}}(\underline{\varphi}(s;0;r)) = \underline{f}(s;r), \quad \overline{\mathcal{L}}(\overline{\varphi}(s;0;r)) = \overline{f}(s;r). \tag{29}$$

The auxiliary function $\tilde{\mathcal{H}}(q;r)$ for equations in (27) are:

$$\begin{cases} \underline{\mathcal{H}}(q;r) = \sum_{j=1}^{\infty} \underline{\mathcal{C}}_j(r) q^j = \underline{\mathcal{C}}_1(r) q^1 + \underline{\mathcal{C}}_2(r) q^2 + \cdots, \\ \overline{\mathcal{H}}(q;r) = \sum_{j=1}^{\infty} \overline{\mathcal{C}}_j(r) q^j = \overline{\mathcal{C}}_1(r) q^1 + \overline{\mathcal{C}}_2(r) q^2 + \cdots, \end{cases} \tag{30}$$

where $\tilde{\mathcal{C}}_1(r) = \left[\underline{\mathcal{C}}_1(r), \overline{\mathcal{C}}_1(r)\right], \tilde{\mathcal{C}}_2(r) = \left[\underline{\mathcal{C}}_2(r), \overline{\mathcal{C}}_2(r)\right], \cdots$ are the auxiliary convergence constants. Expanding the solution $\tilde{\varphi}(s;q;r)$ about q by Taylor's series leads to the series approximate solution via FV-OHAM:

$$\begin{cases} \underline{\phi}(s;q;\underline{\mathcal{C}}_j(r);r) = \underline{v}_0(s;r) + \sum_{j=1}^{\infty} \underline{v}_j(s;\underline{\mathcal{C}}_j(r);r) q^j. \\ \overline{\phi}(s;q;\overline{\mathcal{C}}_j(r);r) = \overline{v}_0(s;r) + \sum_{j=1}^{\infty} \overline{v}_j(s;\overline{\mathcal{C}}_j(r);r) q^j. \end{cases} \tag{31}$$

Substituting equations (30) and (31) into the last two equations of (27), and collecting the coefficient of like powers of q to find the lower and upper bounds yield a system of linear equations. The system for the zeroth order is given in equation (27). The system for the first order are as follows:

$$\begin{cases} \underline{\mathcal{L}}(\underline{v}_1(s;r)) - \underline{\mathcal{L}}(\underline{v}_0(s;r)) + \underline{f}(s) = \underline{\mathcal{C}}_1(r) \left(\underline{\mathcal{L}}(\underline{v}_0(s;r)) - \underline{\lambda}(r) \int_a^t \mathcal{F}_0(\underline{v}_0(s;r)) ds - \underline{f}(s;r) \right), \\ \overline{\mathcal{L}}(\overline{v}_1(s;r)) - \overline{\mathcal{L}}(\overline{v}_0(s;r)) + \overline{f}(s) = \overline{\mathcal{C}}_1(r) \left(\overline{\mathcal{L}}(\overline{v}_0(s;r)) - \overline{\lambda}(r) \int_a^t \mathcal{G}_0(\overline{v}_0(s;r)) ds - \overline{f}(s;r) \right). \end{cases} \tag{32}$$

The problem of second-order is defined as:

$$\begin{cases} \underline{\mathcal{L}}\left(\underline{v}_2(s;r)\right) - \underline{\mathcal{L}}\left(\underline{v}_1(s;r)\right) = \underline{\mathcal{C}}_1(r)\underline{\mathcal{L}}\left(\underline{v}_1(s;r)\right) - \underline{\mathcal{C}}_1(r)\underline{\lambda}(r)\displaystyle\int_a^t \mathcal{F}_1\left(\underline{v}_0(s;r)\right) ds \\ \quad -\underline{\mathcal{C}}_2(r)\underline{\lambda}(r)\displaystyle\int_a^t \mathcal{F}_0\left(\underline{v}_0(s;r)\right) ds - \underline{f}(s;r)\Big], \\ \overline{\mathcal{L}}\left(\overline{v}_2(s;r)\right) - \overline{\mathcal{L}}\left(\overline{v}_1(s;r)\right) = \overline{\mathcal{C}}_1(r)\overline{\mathcal{L}}\left(\overline{v}_1(s;r)\right) - \overline{\mathcal{C}}_1(r)\overline{\lambda}(r)\displaystyle\int_a^t \mathcal{G}_1\left(\overline{v}_0(s;r)\right) ds \\ \quad -\overline{\mathcal{C}}_2(r)\overline{\lambda}(r)\displaystyle\int_a^t \mathcal{G}_0\left(\underline{v}_0(s;r)\right) ds - \overline{f}(s;r)\Big]. \end{cases} \tag{33}$$

The general form of the governing problem via FV-OHAM of k^{th} order:

$$\begin{cases} \underline{\mathcal{L}}\left(\underline{v}_k(s;r)\right) - \underline{\mathcal{L}}\left(\underline{v}_{k-1}(s;r)\right) = \underline{\mathcal{C}}_1(r)\underline{\mathcal{L}}\left(\underline{v}_{k-1}(s;r)\right) + \displaystyle\sum_{i=2}^{k-1}\underline{\mathcal{C}}_i(r)\Big[\underline{\mathcal{L}}\left(\underline{v}_{k-i}(s;r)\right) \\ \quad -\underline{\lambda}(r)\displaystyle\sum_{i=1}^{k}\int_a^s \underline{\mathcal{C}}_i(r)\mathcal{F}_{k-i}\left(\underline{v}_0(s;r),\underline{v}_1(s;r),\ldots,\underline{v}_i(s;r)\right) - \underline{f}(s;r)\Big] \\ \overline{\mathcal{L}}\left(\overline{v}_k(s;r)\right) - \overline{\mathcal{L}}\left(\overline{v}_{k-1}(s;r)\right) = \overline{\mathcal{C}}_1(r)\overline{\mathcal{L}}\left(\overline{v}_{k-1}(s;r)\right) + \displaystyle\sum_{i=2}^{k-1}\overline{\mathcal{C}}_i(r)\Big[\overline{\mathcal{L}}\left(\overline{v}_{k-i}(s;r)\right) \\ \quad -\overline{\lambda}(r)\displaystyle\sum_{i=1}^{k}\int_a^s \overline{\mathcal{C}}_i(r)\mathcal{G}_{k-i}\left(\overline{v}_0(s;r),\overline{v}_1(s;r),\ldots,\overline{v}_i(s;r)\right) - \overline{f}(s;r)\Big] \end{cases} \tag{34}$$

where $\mathcal{F}_{k-i}(\tilde{v}_0(s;r),\tilde{v}_1(s;r),\ldots,\tilde{v}_i(s;r))$ and $\mathcal{G}_{k-i}(\tilde{v}_0(s;r),\tilde{v}_1(s;r),\ldots,\tilde{v}_i(s;r))$ are the coefficients of the lower and upper bound of q^k, respectively. Dependent on parameter $\mathcal{C}_1(r),\mathcal{C}_2(r),\ldots,\mathcal{C}_k(r)$ and at $q=1$ we have:

$$\begin{cases} \underline{v}\left(s,\underline{\mathcal{C}}_1(r),\underline{\mathcal{C}}_2(r),\ldots;r\right) = \underline{v}_0(s;r) + \displaystyle\sum_{i=1}^{\infty}\underline{v}_i\left(s,\underline{\mathcal{C}}_1(r),\underline{\mathcal{C}}_2(r),\ldots;r\right), \\ \overline{v}\left(s,\overline{\mathcal{C}}_1(r),\overline{\mathcal{C}}_2(r),\ldots;r\right) = \overline{v}_0(s;r) + \displaystyle\sum_{i=1}^{\infty}\overline{v}_i\left(s,\overline{\mathcal{C}}_1(r),\overline{\mathcal{C}}_2(r),\ldots;r\right). \end{cases} \tag{35}$$

Approximating the series solution up to the k-th term, Equation (35) becomes:

$$\begin{cases} \underline{v}_*\left(s,\underline{\mathcal{C}}_1(r),\underline{\mathcal{C}}_2(r),\ldots,\underline{\mathcal{C}}_k(r);r\right) = \underline{v}_0(s;r) + \displaystyle\sum_{i=1}^{k}\underline{v}_i\left(s,\underline{\mathcal{C}}_1(r),\underline{\mathcal{C}}_2(r),\ldots,\underline{\mathcal{C}}_i(r);r\right), \\ \overline{v}_*\left(s,\overline{\mathcal{C}}_1(r),\overline{\mathcal{C}}_2(r),\ldots,\overline{\mathcal{C}}_k(r);r\right) = \overline{v}_0(s;r) + \displaystyle\sum_{i=1}^{k}\overline{v}_i\left(s,\overline{\mathcal{C}}_1(r),\overline{\mathcal{C}}_2(r),\ldots,\overline{\mathcal{C}}_i(r);r\right). \end{cases} \tag{36}$$

6. Convergence Analysis of FV-OHAM

Let the residual error be $\tilde{R} = [\underline{R}, \overline{R}]$. Substituting equation (34) into equations (8) and (9) yields [27]:

$$\begin{aligned}
&\underline{R}\left(s, \underline{\mathcal{C}}_1(r), \underline{\mathcal{C}}_2(r), \ldots, \underline{\mathcal{C}}_k(r); r\right) = \\
&\underline{f}\left(s, \underline{\mathcal{C}}_1(r), \underline{\mathcal{C}}_2(r), \ldots, \underline{\mathcal{C}}_i(r); r\right) + \underline{\lambda}(r) \int_a^b K(s,t) v_n\left(t, \underline{\mathcal{C}}_1(r), \underline{\mathcal{C}}_2(r), \ldots, \underline{\mathcal{C}}_k(r)\right) dt, \\
&\overline{R}\left(s, \overline{\mathcal{C}}_1(r), \overline{\mathcal{C}}_2(r), \ldots, \overline{\mathcal{C}}_k(r); r\right) = \\
&\overline{f}\left(s, \overline{\mathcal{C}}_1(r), \overline{\mathcal{C}}_2(r), \ldots, \overline{\mathcal{C}}_i(r); r\right) + \overline{\lambda}(r) \int_a^b K(s,t) v_n\left(t, \overline{\mathcal{C}}_1(r), \overline{\mathcal{C}}_2(r), \ldots, \overline{\mathcal{C}}_k(r)\right) dt.
\end{aligned} \tag{37}$$

For $\tilde{R} = 0$, $\tilde{v}_n$ is the exact solution. To determine the auxiliary constants, $\tilde{\mathcal{C}}_1(r), \tilde{\mathcal{C}}_2(r), \ldots, \tilde{\mathcal{C}}_k(r)$, the least squares method is applied on the interval $s \in [s_0, S]$:

$$\begin{cases}
\underline{M}\left(s, \underline{\mathcal{C}}_1(r), \underline{\mathcal{C}}_2(r), \ldots, \underline{\mathcal{C}}_k(r); r\right) = \displaystyle\int_{s_0}^{s} \underline{R}^2\left(s, \underline{\mathcal{C}}_1(r), \underline{\mathcal{C}}_2(r), \ldots, \underline{\mathcal{C}}_k(r); r\right) ds, \\
\overline{M}\left(s, \overline{\mathcal{C}}_1(r), \overline{\mathcal{C}}_2(r), \ldots, \overline{\mathcal{C}}_k(r); r\right) = \displaystyle\int_{s_0}^{s} \overline{R}^2\left(s, \overline{\mathcal{C}}_1(r), \overline{\mathcal{C}}_2(r), \ldots, \overline{\mathcal{C}}_k(r); r\right) ds,
\end{cases} \tag{38}$$

where s_0 and s are set based on the given problem, $\tilde{M} = [\underline{M}, \overline{M}]$, and the optimal values for $\tilde{C}_1(r), \tilde{C}_2(r), \ldots, \tilde{C}_k(r)$ can be determined for all $r \in [0,1]$ by the following:

$$\frac{\partial \tilde{M}}{\partial \tilde{C}_1} = \frac{\partial \tilde{M}}{\partial \tilde{C}_2} = \cdots = \frac{\partial \tilde{M}}{\partial \tilde{C}_k} = 0. \tag{39}$$

These parameters will be used in the OHAM series solution in equation (21) for each r. This process revolves around minimizing the residual equations. These convergence parameters will then be used to approximate the analytical solution for the FVIEs. Therefore, to find an approximate solution of the FVIE by OHAM, the following steps are followed:

Step 1: Select integers a, b, and n, where $[a, b]$ is the interval and n is the number of iterations.

Step 2: Set $\tilde{x}_0(s,r) = f(s,r)$ as an initial approximation.

Step 3: Calculate the iterations $x_i(s,r)$ in Equation (2) for all $i = 1, 2, \ldots, n$.

Step 4: Compute the partial sum $\tilde{x}_n(s,r) = \sum_{i=0}^{n-1} X_i(s,r)$.

Step 5: If $\tilde{R} = 0$ in equations $(22-32)$, then $\tilde{v}$ produces the exact solution.

Step 6: Determine the optimal values of $\tilde{C}_i$ for $i = 0, \ldots, n$ by applying the least squares minimization approach in equation (25).

Step 7: Compute the absolute error of each root $|v_v exact(s,r) - v_n(s,r)|$.

7. Formulation and Analysis of the Fuzzy Volterra Multistage Optimal Homotopy Asymptotic Method (FV-MOHAM)

MOHAM addresses the limitation of applying OHAM over a single large time interval, where accuracy and convergence often degrade for highly nonlinear or complex problems. When OHAM is applied over a large time interval $[s_0, S][s_0, S][s_0, S]$, the solution may not converge well or may become inaccurate. MOHAM addresses the limitation by subdividing the time interval $[s_0, S]$ into N sub-intervals $[s_0, s_1], \ldots, \ldots, [s_{n-1}, S])$, where each sub-interval employs OHAM. An initial estimation of the solution over the subsequent interval is indicated by the

solution at the terminal point in each sub-interval. This process continues until the predefined time S is reached. FV-MOHAM is implemented similarly to FV-OHAM with minor adjustments. The general initial condition is assumed to be $v_{0,i}(s_i) = \gamma_i, \quad i = 1, \ldots, n$. Therefore, the formulation of the FV-MOHAM equation in each sub-interval is as follows [27, 33]:

$$(1-q)\left[\tilde{\mathcal{L}}_i(\tilde{\varphi}_i(s;q;r)) - \tilde{f}(s;r)\right] = \tilde{\mathcal{H}}_i(q;r)\left[\tilde{\mathcal{L}}(\tilde{\varphi}_i(s;q;r)) - \tilde{k}_i(s,\tilde{v}_i(s;r)) - \tilde{f}(s;r)\right]. \tag{40}$$

Hence, the dynamic of FV-MOHAM is:

$$\begin{cases} \underline{\mathcal{L}}_i(\underline{v}_i(s;r)) - \mathcal{F}_i(s,\tilde{v}_i(s;r)) - \underline{f}(s;r) = 0, \\ \overline{\mathcal{L}}_i(\overline{v}_i(s;r)) - \mathcal{G}_i(s,\tilde{v}(s;r)) - \overline{f}(s;r) = 0, \\ (1-q)\left[\underline{\mathcal{L}}_i(\underline{\varphi}_i(s;q;r)) - \underline{f}(s;r)\right] = \underline{\mathcal{H}}_i(q;r)\left[\underline{\mathcal{L}}_i(\underline{\varphi}_i(s;q;r)) - \mathcal{F}_i(s,\tilde{v}_i(s;r)) - \underline{f}(s;r)\right], \\ (1-q)\left[\overline{\mathcal{L}}_i(\overline{\varphi}_i(s;q;r)) - \overline{f}(s;r)\right] = \overline{\mathcal{H}}_i(q;r)\left[\overline{\mathcal{L}}_i(\overline{\varphi}_i(s;q;r)) - \mathcal{G}_i(s,\tilde{v}_i(s;r)) - \overline{f}(s;r)\right]. \end{cases} \tag{41}$$

When $q = 0$ and $q = 1$, we respectively have:

$$\begin{aligned} \underline{\varphi}_i(s;0;r) &= \underline{v}_{0,i}(s;r), \ \underline{\varphi}_i(s;1;r) = \underline{v}_i(s;r), \\ \overline{\varphi}_i(s;0;r) &= \overline{v}_{0,i}(s;r), \ \overline{\varphi}_i(s;1;r) = \overline{v}_i(s;r), \end{aligned} \tag{42}$$

where the lower and upper bounds of the zeroth order respectively are:

$$\underline{\mathcal{L}}_i(\underline{\varphi}_i(s;0;r)) = \underline{f}(s;r), \overline{\mathcal{L}}_i(\overline{\varphi}_i(s;0;r)) = \overline{f}(s;r), \tag{43}$$

and the auxiliary function $\tilde{\mathcal{H}}_i(q;r)$ for equations (37) and (38) are:

$$\begin{cases} \underline{\mathcal{H}}_i(q;r) = \sum_{j=1}^{\infty} \underline{C}_{j,i}(r) q^j = \underline{C}_{1,i}(r) q^1 + \underline{C}_{2,i}(r) q^2 + \cdots, \\ \overline{\mathcal{H}}_i(q;r) = \sum_{j=1}^{\infty} \overline{C}_{j,i}(r) q^j = \overline{C}_{1,i}(r) q^1 + \overline{C}_{2,i}(r) q^2 + \cdots. \end{cases} \tag{44}$$

The series approximate solutions of FV-MOHAM then become:

$$\begin{cases} \underline{\varphi}_i\left(s;q;\underline{C}_{j,i}(r);r\right) = \underline{v}_{0,i}(s;r) + \sum_{j=1}^{\infty} \underline{v}_{j,i}(s;\underline{C}_{j,i}(r);r) q^j, \\ \overline{\varphi}_i\left(s;q;\overline{C}_{j,i}(r);r\right) = \overline{v}_{0,i}(s;r) + \sum_{j=1}^{\infty} \overline{v}_j(s;\overline{C}_j(r);r) q^j. \end{cases} \tag{45}$$

Substituting equations (44) and (45) into the last two of equation (41) and collecting the coefficient of like powers of q yield a system of linear equations. The zeroth-order system is given in equation (41) whereas the first is as follows:

$$\begin{cases} \underline{\mathcal{L}}_i\left(\underline{v}_{1,i}(s;r)\right) - \underline{\mathcal{L}}_i\left(\underline{v}_{0,i}(s;r)\right) + \underline{f}(s) = \underline{C}_{1,i}(r)\left(\underline{\mathcal{L}}_i\left(\underline{v}_{0,i}(s;r)\right) - \underline{\lambda}(r)\int_a^t \mathcal{F}_{0,i}\left(\underline{v}_{0,i}(s;r)\right) ds - \underline{f}(s;r)\right), \\ \overline{\mathcal{L}}_i\left(\overline{v}_{1,i}(s;r)\right) - \overline{\mathcal{L}}_i\left(\overline{v}_{0,i}(s;r)\right) + \overline{f}(s) = \overline{C}_{1,i}(r)\left(\overline{\mathcal{L}}_i\left(\overline{v}_{0,i}(s;r)\right) - \overline{\lambda}(r)\int_a^t \mathcal{G}_{0,i}\left(\overline{v}_{0,i}(s;r)\right) ds - \overline{f}(s;r)\right). \end{cases} \tag{46}$$

The general form of the governing problem via FV-OHAM of k^{th} order is:

$$\begin{cases} \underline{\mathcal{L}}\left(\underline{v}_k(s;r)\right) - \underline{\mathcal{L}}_i\left(\underline{v}_{k-1,i}(s;r)\right) = \underline{C}_{1,i}(r)\underline{\mathcal{L}}_i\left(\underline{v}_{k-1,i}(s;r)\right) + \sum_{j=2}^{k-1}\underline{C}_{j,i}(r)\left[\underline{\mathcal{L}}_i\left(\underline{v}_{k-j,i}(s;r)\right)\right. \\ \left. - \underline{\lambda}(r)\sum_{j=1}^{k}\int_a^s \underline{C}_{j,i}(r)\underline{\mathcal{F}}_{k-j,i}\left(\underline{v}_{0,i}(s;r),\underline{v}_{1,i}(s;r),\ldots,\underline{v}_{j,i}(s;r)\right) - \underline{f}(s;r)\right], \\ \overline{\mathcal{L}}_i\left(\overline{v}_{k,i}(s;r)\right) - \overline{\mathcal{L}}_i\left(\overline{v}_{k-1,i}(s;r)\right) = \overline{C}_{1,i}(r)\overline{\mathcal{L}}_i\left(\overline{v}_{k-1,i}(s;r)\right) + \sum_{j=2}^{k-1}\overline{C}_{j,i}(r)\left[\,\overline{\mathcal{L}}_i\left(\underline{v}_{k-j,i}(s;r)\right)\right. \\ \left. - \overline{\lambda}(r)\sum_{j=1}^{k}\int_a^s \overline{C}_i(r)\mathcal{G}_{k-j,i}\left(\overline{v}_{0,i}(s;r),\overline{v}_{1,i}(s;r),\ldots,\overline{v}_{j,i}(s;r)\right) - \overline{f}(s;r)\,\right], \end{cases} \tag{47}$$

where $\mathcal{F}_{k-j,i}\left(\tilde{v}_{0,i}(s;r),\tilde{v}_{1,i}(s;r),\ldots,\tilde{v}_{j,i}(s;r)\right)$ and $\mathcal{G}_{k-j,i}\left(\tilde{v}_{0,i}(s;r),\tilde{v}_{1,i}(s;r),\ldots,\tilde{v}_{j,i}(s;r)\right)$ are the coefficients of the lower and upper bound of q^k, respectively. Dependent on parameter $C_{1,i}(r), C_{2,i}(r),\ldots,C_{k,i}(r)$, at $q=1$ we have:

$$\begin{cases} \underline{v}_i(s,\underline{C}_{1,i}(r),\underline{C}_{2,i}(r),\ldots;r) = \underline{v}_{0,i}(s;r) + \sum_{j=1}^{\infty}\underline{V}_{j,i}(s,\underline{C}_{1,i}(r),\underline{C}_{2,i}(r),\ldots;r), \\ \overline{v}_i(s,\overline{C}_{1,i}(r),\overline{C}_{2,i}(r),\ldots;r) = \overline{v}_{0,i}(s;r) + \sum_{j=1}^{\infty}\overline{v}_{j,i}(s,\overline{C}_{1,i}(r),\overline{C}_{2,i}(r),\ldots;r). \end{cases} \tag{48}$$

Approximating the series solution up to the kth term yield:

$$\begin{cases} \underline{v}_{*,i}(s,\underline{C}_{1,i}(r),\underline{C}_{2,i}(r),\ldots,\underline{C}_{k,i}(r);r) = \underline{v}_{0,i}(s;r) + \sum_{j=1}^{k}\underline{v}_{j,i}(s,\underline{C}_{1,i}(r),\underline{C}_{2,i}(r),\ldots,\underline{C}_{j,i}(r);r), \\ \overline{v}_{*,i}(s,\overline{C}_{1,i}(r),\overline{C}_{2,i}(r),\ldots,\overline{C}_{k,i}(r);r) = \overline{v}_{0,i}(s;r) + \sum_{j=1}^{k}\overline{v}_{j,i}(s,\overline{C}_{1,i}(r),\overline{C}_{2,i}(r),\ldots,\overline{C}_{j,i}(r);r). \end{cases} \tag{49}$$

The residual error $\tilde{R}_i$ can then be computed as follows:

$$\begin{cases} \underline{R}_i\left(s,\underline{C}_{j,i}(r);r\right) = \underline{f}(s,\underline{C}_{j,i}(r);r) + \underline{\lambda}(r)\int_a^b K(s,t)v_{n,i}(t,\underline{C}_{j,i}(r)dt, \\ \overline{R}_i\left(s,\underline{C}_{j,i}(r);r\right) = \overline{f}(s,\overline{C}_{j,i}(r);r) + \overline{\lambda}(r)\int_a^b K(s,t)v_{n,i}(t,\underline{C}_{j,i}(r)dt. \end{cases} \tag{50}$$

For $\tilde{R}_i = 0$, $\tilde{v}_{*,i}$ yields the exact solution. To determine the auxiliary constants $\tilde{C}_{j,i}$, the least squares method is applied on the interval $s \in [s_0, S]$:

$$\begin{cases} \underline{M}_i\left(s,\underline{C}_{j,i}(r);r\right) = \int_{s_i}^{s_i+h}\underline{R}^2\left(s,\underline{C}_{j,i}(r);r\right)ds, \\ \overline{M}_i\left(s,\overline{C}_{j,i}(r);r\right) = \int_{s_i}^{s_i+h}\overline{R}^2\left(s,\overline{C}_{j,i}(r);r\right)ds, \end{cases} \tag{51}$$

where h is the length of the sub-interval $[s_i, s_{i+1})$, and $n = S/h$ is the number of sub-intervals. Equation (46) can now be solved at $i = 1,\ldots,n$ and $j = 1,\ldots,k$ by altering the starting estimate γ_i in each subinterval from

its predecessor. The unidentified convergence control parameters $C_{j,i}$ can be determined by solving the following system of equations:

$$\frac{\partial \tilde{M}_i}{\partial \tilde{C}_{1,i}} = \frac{\partial \tilde{M}_i}{\partial \tilde{C}_{2,i}} = \cdots = \frac{\partial \tilde{M}_i}{\partial \tilde{C}_{k,i}} = 0. \tag{52}$$

Therefore, the approximate analytical solution for the FVIE is:

$$\tilde{v}(s) = \begin{cases} \tilde{v}_1(s), & s_0 \leq s \leq s_1 \\ \tilde{v}_2(s), & s_1 \leq s \leq s_2 \\ \cdots & \cdots\cdots \\ \tilde{v}_n(s), & s_{n-1} \leq s \leq S \end{cases} \tag{53}$$

In this way, the analytical solution can correctly be derived for the initial value issue at high values of S. FV-MOHAM reduces to the conventional FV-OHAM when $i = 0$. FV-MOHAM offers an easy method of regulating and modifying the convergence zone via the auxiliary function $\mathcal{H}_i(q)$ and several convergent control parameters $C_{j,i}$. However, this approach primarily addresses the challenge of locating an approximation for a problem with a vast domain. According to Gomes et al. [26], both series in equations (32) and (48) converge for each r-level set core which corresponds to the solution of equation (4).

8. Examples

In this section, two second-kind linear FVIEs are solved using FV-OHAM and FV-MOHAM. The corresponding execution, results, and analysis are presented. The absolute error, $\tilde{E}r$, and the mean error, $\tilde{M}_{Er}$, are defined as follows:

$$\tilde{E}r(t,r) = |\widetilde{XX}(t;r) - \tilde{X}(t;r)| = \begin{cases} |\underline{XX}(t;r) - \underline{X}(t;r)| \\ |\overline{XX}(t;r) - \overline{X}(t;r)|, \end{cases} \tag{54}$$

$$\tilde{M}_{Er}(t,r) = \frac{\underline{Er}(t,r) + \overline{Er}(t,r)}{2}, \tag{55}$$

where $\tilde{X}(t;r)$ refers to the exact solution of the given problem, and $\widetilde{XX}(t;r)$ is the approximate solution generated by the FV-OHAM and FV-MOHAM corresponding to the given problem for $r \in [0,1]$. Throughout this paper, X represents the exact solution whereas x, $\overline{X}$, and $\underline{X}$ denote the approximate, upper exact, and lower exact solutions, respectively.

8.1. Example 1

Consider the following linear FVIE [33]:

$$\tilde{x}(t) = \tilde{f}(t) + \int_0^t e^{(t-s)}\tilde{x}(s)ds, \tag{56}$$

where

$$\tilde{f}(t;r) = (\cos t)\,[r, 2-r]. \tag{57}$$

The exact solution is given by

$$\tilde{X}(t;r) = [r, 2-r](\frac{3}{5}\cos t + \frac{1}{5}sint + \frac{2}{5}e^{2t}). \tag{58}$$

To determine the lower bound of the residual error and solve Example 1 using FV-OHAM with the sixth iteration, the initial approximations for all $r \in [0,1]$ are first chosen based on the method analysis in sections 4 and 5. The FV-OHAM formulation for equation (56) is:

$$H(x) = (1-p)[x(t) - \tilde{x}_0(t)] + p[x(t) - [r, 2-r]\cos t - \lambda \int_0^t e^{(t-s)}\tilde{x}(s)ds] = 0, \tag{59}$$

where $p \in [0,1]$ is an embedding parameter, $\tilde{x_0}(t)$ is the zeroth approximation solutions. The expansion of $\tilde{x}$ in powers of p,

$$\tilde{x}(t) = \tilde{x}_0(t) + p\tilde{x}_1(t) + p^2\tilde{x}_2(t) + \ldots\ldots\ldots\ldots\ldots\ldots + p^n\tilde{x}_n(t), \tag{60}$$

is substituted into Equation (59),

$$\begin{aligned} H(x,p) = (1-p)\left[\sum_{i=0}^{n} p^i\tilde{x}_i(t) - \tilde{x}_0(t)\right] + p\left[\sum_{i=0}^{n} p^i\tilde{x}_i(t) - [r,2-r]\cos t - \right. \\ \left. \lambda\int_a^t e^{(t-s)}\sum_{i=0}^{n} p^i x_i(s)ds\right] = 0. \end{aligned} \tag{61}$$

Therefore, the zeroth, first, and m-th order approximations can be determined and are presented in equations (62), (63), and (64), respectively.

$$\tilde{x}(t)_0 = [r, 2-r]\cos t, \tag{62}$$

$$\tilde{x}_1(t) = [r,2-r]\left[-C_1\int_0^t (t-s)\tilde{x}_0(s)ds\right] = [r,2-r][2e^t\cos t - 2\cos t], \tag{63}$$

$$\tilde{x}_m(t) = [r,2-r][(1+C_1)\tilde{x}_{m-1}(t) + \sum_{k=1}^{m-1} C_k\tilde{x}_{m-k}(t) - \sum_{k=1}^{m} c_{1,k}\int_0^t e^{(t-s)}\tilde{x}_{m-k}(s)ds]. \tag{64}$$

As discussed in sections 4 and 5, the convergence control parameters for FV-OHAM for this example were calculated and tabulated in tables 1 and 2 for different values of $r \in [0,1]$ and $t = \frac{\pi}{8}$. The parameters were then used to generate the sixth-order approximate solutions for Example 1. Table 3 presents the numerical and exact solutions, whereas figures 1 and 2 display their two- and three-dimensional plots, respectively. Lastly, Table 4 records the absolute and mean errors of the results.

Table 1. Optimal convergence parameters of the sixth-order FV-OHAM for the lower solution of Example 1 at selected values of $r \in [0,1]$ and $t = \frac{\pi}{8}$.

r	$\underline{C}_1$	$\underline{C}_2$	$\underline{C}_3$	$\underline{C}_4$	$\underline{C}_5$	$\underline{C}_6$
0	-1	0	0	0	0	0
0.2	-1.06375297327059	0.0254386028843473	-0.0084311631572610	0.000609600820668207	0.000248232291041695	-0.000037493712259645 0
0.4	-1.06375297325867	0.0254386029035415	-0.0084311631637278	0.000609600819894774	0.000248232291769420	-0.000037493712343956 3
0.6	-1.06375297314049	0.0254386027787727	-0.0084311631172603	0.000609600816778696	0.000248232289245485	-0.000037493710821075 9
0.8	-1.06375297331381	0.0254386028935962	-0.0084311631511059	0.000609600817764054	0.000248232291209059	-0.000037493712148079 7
1	-1.06375297236219	0.0254386028384862	-0.0084311632746214	0.000609600853995687	0.000248232293860045	-0.000037493713703780 5

Table 2. Optimal convergence parameters of the sixth-order FV-OHAM for the upper solution of Example 1 at selected values of $r \in [0, 1]$ and $t = \frac{\pi}{8}$.

r	$\overline{C}_1$	$\overline{C}_2$	$\overline{C}_3$	$\overline{C}_4$	$\overline{C}_5$	$\overline{C}_6$
0	-1.06375297286719	0.0254386028446668	-0.0084311632067809	0.00060960083641758	0.000248232292178112	-0.00003749371266644
0.2	-1.06375297330467	0.0254386029801644	-0.0084311632038488	0.00060960082872342	0.000248232291739776	-0.00003749371162798
0.4	-1.06375297314607	0.0254386028935392	-0.0084311631776690	0.00060960082412600	0.000248232292166044	-0.00003749371270290
0.6	-1.06375297329602	0.0254386029448837	-0.0084311631891171	0.00060960082393238	0.000248232293193404	-0.00003749371262592
0.8	-1.06375297315491	0.0254386028081106	-0.0084311631235094	0.00060960081510175	0.000248232290095667	-0.00003749371082786
1	-1.06375297285611	0.0254386029862732	-0.0084311632434452	0.00060960082922808	0.000248232296712564	-0.00003749371302230

Table 3. Sixth order FV-OHAM numerical and exact solutions for Example 1 at $t = \frac{\pi}{8}$.

r	$\underline{X}_{lower\,\boldsymbol{OHAM}}$	$\underline{x}_{lower\,\boldsymbol{OHAM}}$	$\overline{X}_{upper\,\boldsymbol{OHAM}}$	$\overline{x}_{upper\,\boldsymbol{OHAM}}$
0	0	0	3.0163528525499923	3.0163527684815534
0.2	0.3016352852549993	0.3016352768481554	2.714717567294993	2.7147174916333983
0.4	0.6032705705099985	0.6032705536963108	2.413082282039994	2.413082214785243
0.6	0.9049058557649978	0.9049058305444662	2.1114469967849945	2.111446937937087
0.8	1.206541141019997	1.2065411073926215	1.8098117115299952	1.8098116610889319
1	1.5081764262749962	1.5081763842407767	1.5081764262749962	1.5081763842407767

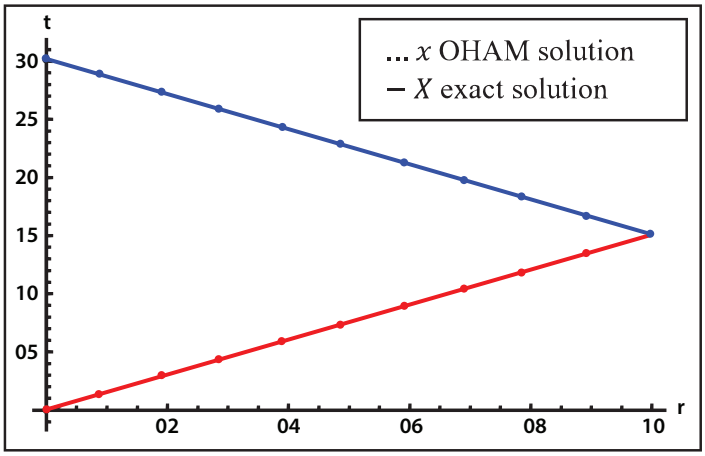

Figure 1. The approximate solutions (upper and lower) for Example 1 using sixth-order FV-OHAM at $t = \frac{\pi}{8}$ and the exact solutions.

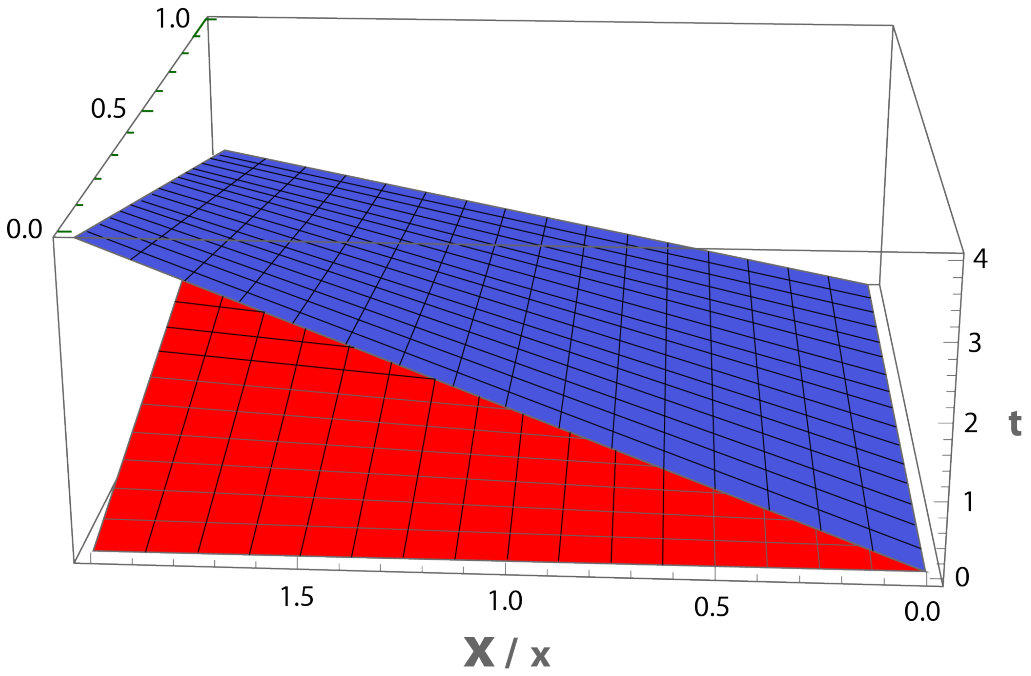

Figure 2. Three-dimensional plots of the approximate solutions (upper and lower) for Example 1 using sixth-order FV-OHAM at $t = \frac{\pi}{8}$ and the exact solutions.

Table 4. The absolute and mean errors of the sixth-order FV-OHAM for Example 1.

r	$\underline{E}r(t,r)$	$\overline{E}r(t,r)$	$\widetilde{M}E(t,r)$
0	0	8.40684×10^{-8}	4.203450×10^{-8}
0.2	8.40684×10^{-9}	7.56616×10^{-8}	4.203442×10^{-8}
0.4	1.68137×10^{-8}	6.72548×10^{-8}	4.203430×10^{-8}
0.6	2.52205×10^{-8}	5.88479×10^{-8}	4.203425×10^{-8}
0.8	3.36274×10^{-8}	5.04411×10^{-8}	4.203425×10^{-8}
1	4.20342×10^{-8}	4.20342×10^{-8}	4.203420×10^{-8}

Applying the FV-MOHAM at $j = 1$, the initial approximation is taken as:

$$\tilde{X}(t)_{1,0} = 0. \tag{65}$$

The corresponding homotopy is constructed as follows:

$$\begin{aligned} \tilde{x}(t)_{1,1} &= (c_{1,1,1} + c_{1,2,1}t + c_{1,3,1}t^2)[\tilde{x}(t)_0 - r(\cos(t)) - \int_0^t e^{(t-s)}\tilde{x}(s)_{1,0}ds] \\ &= (c_{1,1} + c_{1,2}t + c_{1,3}t^2)(-r(\cos(t))), \end{aligned} \tag{66}$$

whereby the first approximation is

$$\tilde{H}(t)_{1,1} = \tilde{x}(t)_{1,0} + \tilde{x}(t)_{1,1} = (c_{1,1,1} + c_{1,2,1}t + c_{1,3,1}t^2)(-r(\cos(t))), \tag{67}$$

with residual function,

$$R_{1,1} = \tilde{x}(t)_{1,1} - r(\cos(t)) - \int_0^t e^{(t-s)}\tilde{x}(s)_{1,1}ds. \tag{68}$$

By solving for the coefficients and completing the solution with the same steps for $j = 2, 3, 4, 5$, results from FV-MOHAM can be generated. The convergence control parameters for FV-MOHAM are presented in tables 5 and 6, the sixth-order numerical and exact solutions are in Table 7, and the absolute and mean errors of the results are in Table 8. Figures 3 and 4 display the two- and three-dimensional plots of the results, respectively.

Table 5. Optimal convergence parameters of the sixth-order FV-MOHAM for the lower solution of Example 1 at $r \in [0, 1]$.

j	$\underline{C}^j_{11}$	$\underline{C}^j_{12}$	$\underline{C}^j_{13}$	$\underline{C}^j_{21}$	$\underline{C}^j_{22}$	$\underline{C}^j_{23}$
1	-1	0	0	0	0	0
2	-1.004997109552217	0.0001268063881206017	-0.000001231528837	$-3.737701136 \times 10^{-8}$	$8.020468757 \times 10^{-10}$	$-1.27250165 \times 10^{-12}$
3	-1.004668947226675	0.0001171112073488369	-0.000001065122970	$-3.911179170 \times 10^{-8}$	$8.2817171242 \times 10^{-10}$	$-2.06948873 \times 10^{-12}$
4	-1.002938912798394	0.0000070824541371671	0.000001977238771	$-1.026760703 \times 10^{-7}$	$2.3695470747 \times 10^{-9}$	$-3.60044560 \times 10^{-11}$
5	-1.001360191781939	0.0000477260843769630	-0.000001297485588	$3.9804360648 \times 10^{-8}$	$-2.0931484101 \times 10^{-9}$	$5.97316394 \times 10^{-11}$

Table 6. Optimal convergence parameters of the sixth-order FV-MOHAM for the upper solution of Example 1 at $r \in [0, 1]$.

j	$\overline{C}^j_{11}$	$\overline{C}^j_{12}$	$\overline{C}^j_{13}$	$\overline{C}^j_{21}$	$\overline{C}^j_{22}$	$\overline{C}^j_{23}$
1	-1.00124633946281	0.00004722258490787	-0.00000156979876	$5.9143337456 \times 10^{-8}$	$-2.72804467008 \times 10^{-9}$	$7.113291090 \times 10^{-11}$
2	-1.00244251140493	0.00002471881194694	0.0000011725124923	$-8.584147276 \times 10^{-8}$	$1.8974134438167 \times 10^{-9}$	$-2.32234533 \times 10^{-11}$
3	-1.00493826643921	0.00012518137905866	-0.000001202220626	$-3.794406538 \times 10^{-8}$	$8.152356580547 \times 10^{-10}$	$-1.53621470 \times 10^{-12}$
4	-1.00132606066623	-0.00000474402396247	0.0000020583380585	$-1.264650605 \times 10^{-7}$	$3.2864927602941 \times 10^{-9}$	$-5.18421316 \times 10^{-11}$
5	-1.0024763958790825	0.00001748919676085117 8	0.00000155552472206896 3	$-1.028328420 \times 10^{-7}$	$2.4882302221067 \times 10^{-9}$	$-3.54804048 \times 10^{-11}$

Table 7. Sixth order FV-MOHAM numerical and exact solutions for Example 1 with $h = 0.1$, $t = \frac{\pi}{8}$, and $r \in [0, 1]$.

r	$\underline{X}_{MOHAM}$	$\underline{x}_{MOHAM}$	$\overline{X}_{MOHAM}$	$\overline{x}_{MOHAM}$
0	0	0	3.0163528525499923	3.016352852782677
0.2	0.3016352852549993	0.3016352852782677	2.714717567294993	2.714717567504409
0.4	0.6032705705099985	0.6032705705565354	2.413082282039994	2.4130822822261417
0.6	0.9049058557649978	0.9049058558348032	2.1114469967849945	2.1114469969478735
0.8	1.206541141019997	1.2065411411130709	1.8098117115299952	1.809811711669606
1	1.5081764262749962	1.5081764263913384	1.5081764262749962	1.5081764263913384

Table 8. The absolute and mean errors of the sixth-order FV-MOHAM for Example 1 with $h = 0.1, t = \frac{\pi}{8}, r \in [0, 1]$.

r	$\underline{E}_r(t, r)$	$\overline{E}_r(t, r)$	$\widetilde{M}E(t, r)$
0	0	2.32685×10^{-10}	$1.1634250 \times 10^{-10}$
0.2	2.32684×10^{-11}	2.09416×10^{-10}	$1.1634220 \times 10^{-10}$
0.4	4.65369×10^{-11}	1.86148×10^{-10}	$1.1634245 \times 10^{-10}$
0.6	6.98054×10^{-11}	1.62879×10^{-10}	$1.1634220 \times 10^{-10}$
0.8	9.30738×10^{-11}	1.39611×10^{-10}	$1.1634240 \times 10^{-10}$
1	1.16342×10^{-10}	1.16342×10^{-10}	$1.1634200 \times 10^{-10}$

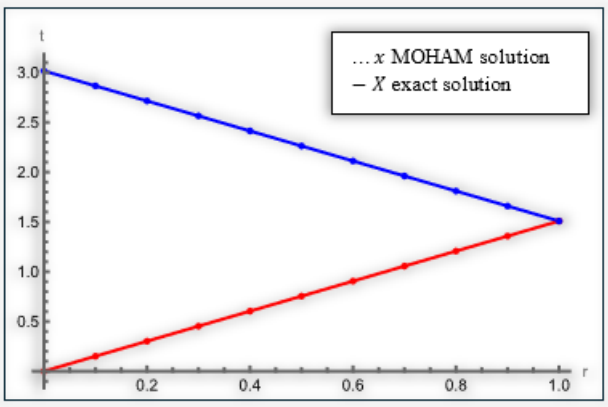

Figure 3. The approximate solutions (upper and lower) for Example 1 using sixth-order FV-MOHAM with $t = \frac{\pi}{8}$, $h = 0.4$, and $r \in [0, 1]$ together with the exact solutions.

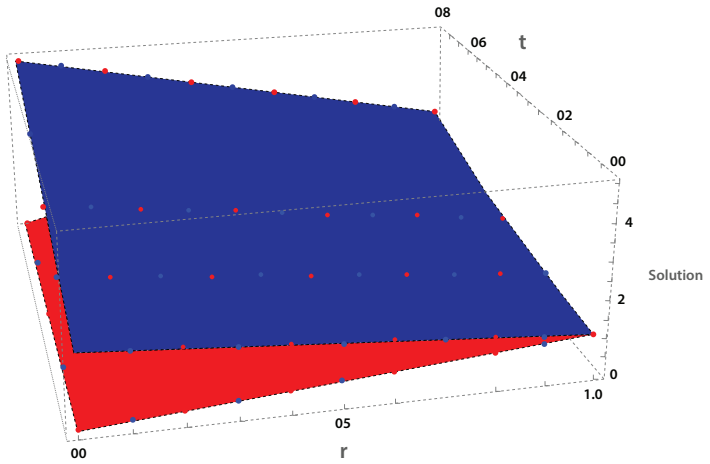

Figure 4. Three-dimensional plots of the approximate solutions (upper and lower) for Example 1 using sixth-order FV-MOHAM with $t = \frac{\pi}{8}$, $h = 0.4$, and $r \in [0, 1]$ together with the exact solutions.

Table 9 provides a comparison of the mean errors of the sixth-order solutions for Example 1 by FV-OHAM, FV-MOHAM, and HAM. The table presents the mean error at $t = \frac{\pi}{8}$ for all three methods over the same range of $r \in [0, 1]$, offering a clear comparison of their performance. Results form Taylor method and variational iteration method (VIM) are also included. From the table, the numerical results computed using sixth-order FV-MOHAM and FV-OHAM significantly outperform those obtained using the sixth-order HAM, Taylor method and VIM at the same values of $r \in [0, 1]$ and $t = \frac{\pi}{8}$. The table shows that both FV-MOHAM and FV-OHAM provide highly accurate solutions, but FV-MOHAM shows a clear superiority in reducing numerical errors over the entire range of r.

Table 9. Mean errors of results from the sixth-order FV-OHAM, FV-MOHAM, and HAM, together with Taylor method and VIM for Example 1 at $t = \frac{\pi}{8}$ for $r \in [0, 1]$.

r	FV-OHAM	FV-MOHAM	HAM [27]	Taylor [27]	VIM [27]
0	4.203450×10^{-8}	$1.1634250 \times 10^{-10}$	$4.05033280470 \times 10^{-7}$	3.4210×10^{-6}	8.4600×10^{-6}
0.2	4.203442×10^{-8}	$1.1634220 \times 10^{-10}$	$4.05033280304 \times 10^{-7}$	3.0790×10^{-6}	7.6100×10^{-6}
0.4	4.203430×10^{-8}	$1.1634245 \times 10^{-10}$	$4.05033280359 \times 10^{-7}$	2.7360×10^{-6}	6.7700×10^{-6}
0.6	4.203425×10^{-8}	$1.1634220 \times 10^{-10}$	$4.05033280637 \times 10^{-7}$	2.3950×10^{-6}	5.9300×10^{-6}
0.8	4.203425×10^{-8}	$1.1634240 \times 10^{-10}$	$4.05033280359 \times 10^{-7}$	2.0520×10^{-6}	5.0700×10^{-6}
1	4.203420×10^{-8}	$1.1634200 \times 10^{-10}$	$4.05033280581 \times 10^{-7}$	1.7104×10^{-6}	4.2400×10^{-6}

While FV-OHAM remains accurate, FV-MOHAM has a higher ability to improve accuracy due to its use of multi stages providing additional improvements to the solutions compared to FV-OHAM. FV-MOHAM applies multiple iteration strategies to improve the accuracy of the solutions. The equation is divided into multiple sub-intervals, which helps in providing more stable and accurate solutions. On the other hand, FV-OHAM relies only on one stage, which makes it less capable in improving solutions compared to FV-MOHAM. As for the HAM method, it produces significantly larger errors, which reflects its lower accuracy when solving linear FVIE of second kind. The Taylor method and the VIM also fall short in terms of the mean errors. The VIM may provide relatively accurate solutions using order higher than six but it is more time-consuming and less efficient compared to both FV-OHAM and FV-MOHAM. Overall, for Example 1, FV-MOHAM generated the most accurate results compared to FV-OHAM, HAM, Taylor method, and VIM.

8.2. Example 2

Consider the following linear Volterra–Hammerstein integral equation [34]:

$$\tilde{X}(t) = \tilde{g}(t) + \int_0^t t\cos(s-t)\tilde{X}(s)ds, \tag{69}$$

where

$$\underline{\tilde{g}}(t;r) = 2t(r^5 + 2r)(3 - 3\cos(t) - t^2), \tag{70}$$

$$\overline{\tilde{g}}(t;r) = 2t(6 - 6r^3)(3 - 3\cos(t) - t^2), \tag{71}$$

and the exact solution,

$$[\underline{\tilde{X}}(t;r), \overline{\tilde{X}}(t;r)] = [t^3(r^5 + 2r), t^3(6 - 6r^3)]. \tag{72}$$

To determine the lower bound of the residual error and solve Example 2 using FV-OHAM with the fourth iteration, the initial approximations for all $r \in [0,1]$ are first chosen based on the method analysis in sections 3 and 5. The FV-OHAM formulation for equation (69) is:

$$H(X) = (1-P)[\tilde{X} - X_0(t)] + P[X - [(r^5+2r),(6-6r^3)](2t(3-3\cos(t)-t^2)) - \lambda \int_0^t (t\cos(s-t))\tilde{X}(s)ds] = 0. \tag{73}$$

The expansion of $\tilde{X}(t)$ in powers of p,

$$\tilde{X}(t) = \tilde{X}_0(t) + \tilde{P}X_1(t) + \tilde{P^2}X_2(t) + \cdots + \tilde{P^n}X_n(t) \tag{74}$$

is substituted into Equation (73),

$$H(X,P) = (1-P)[\sum_{i=0}^{n} \tilde{P^i}X_i(t) - \tilde{X_0}(t)] + P[\sum_{i=0}^{n} \tilde{P^i}X_i(t) - [(r^5+2r),(6-6r^3)](2t(3-3\cos(t)-t^2)) - \lambda \int_a^t (t\cos(s-t))\sum_{i=0}^{n} P^iX_i(s)ds] = 0. \tag{75}$$

Therefore, the initial, first, and m-th order approximations can be determined and are presented in equations (76), (77), and (78), respectively.

$$\tilde{X}(t)_0 = [(r^5+2r),(6-6r^3)](2t(3-3\cos(t)-t^2)). \tag{76}$$

$$\tilde{X_1}(t) = -C_1 \int_0^t (t\cos(s-t))\tilde{X_0}(s)ds. \tag{77}$$

$$\tilde{x}_m(t) = (1+C_1)\tilde{x}_{m-1}(t) + \sum_{k=1}^{m-1} C_k\tilde{x}_{m-k}(t) - \sum_{k=1}^{m} c_{1,k}\int_0^t (t\cos(s-t))\tilde{x}_{m-k}(S)ds. \tag{78}$$

As discussed in sections 3 and 5, the convergence control parameters for FV-OHAM for this example were calculated and tabulated in tables 10 and 11 for different values of $r \in [0,1]$ on interval $0 \le t \le 0.5$. These parameters were then used to generate the fourth-order approximate solutions for Example 2. Tables 12 and 13 displays the numerical solutions and their errors while Figure 5 plots the approximate and exact solutions.

Table 10. Optimal convergence parameters of the fourth-order FV-OHAM method for the lower solution of Example 2 at selected values of $r \in [0,1]$, and $t = 0.5$.

r	$\underline{C_1}$	$\underline{C_2}$	$\underline{C_3}$
0	-1	0	0
0.1	-0.47669646109559977	-0.30071701013081420	0
0.2	-0.55155272972664440	-0.21040081566865340	0
0.3	-0.51259522865766590	-0.24900211629660518	0
0.4	-0.46021287825845597	-0.31410403377279655	0
0.5	-0.51259522865766590	-0.24900211629660518	0

Table 11. Optimal convergence parameters of the fourth-order FV-OHAM method for the upper solution of Example 2 at selected values of $r \in [0, 1]$, and $t = 0.5$.

r	$\overline{C}_1$	$\overline{C}_2$	$\overline{C}_3$
0	-1.08472971176231670	-0.001818326205830011	0
0.1	-0.86479788665404440	-0.011783106983511564	0
0.2	-0.60537179349533940	-0.153801796343688820	0
0.3	-0.59993337053279270	-0.161471060045731900	0
0.4	-0.46713338890094924	-0.306385035384228230	0
0.5	-0.48186648012081740	-0.295300195952291460	0

Table 12. Fourth-order lower FV-OHAM solution for Example 2 at $t = 0.5$ for all $r \in [0, 1]$ and their errors.

r	$\underline{X}_{lowerOHAM}$	$\underline{X}_{lowerOHAM}$	$\underline{E}r(t, r)$
0	0	0	0
0.25	0.0626220703125	0.06262207463774630	$2.1584101445894 \times 10^{-9}$
0.5	0.1289062500000	0.12890625890343096	$4.3168295412585 \times 10^{-9}$
0.75	0.2171630859375	0.21716310093674593	$6.4752241158997 \times 10^{-9}$
1	0.3750000000000	0.37500002590089010	$8.6336311339854 \times 10^{-9}$

Table 13. Fourth-order upper FV-OHAM solution for Example 2 at $t = 0.5$ for all $r \in [0, 1]$ and their errors.

r	$\overline{X}_{upperOHAM}$	$\overline{X}_{upperOHAM}$	$\overline{E}r(t, r)$
0	0.7500000518017	0.7500000518017802	0
0.25	0.7441406250000	0.7441406763970788	2.15841×10^{-9}
0.5	0.7031250000000	0.7031250485641689	4.31682×10^{-9}
0.75	0.5917968750000	0.5917969158748422	6.47522×10^{-9}
1	0.3750000000000	0.3750000259008901	8.63363×10^{-9}

Applying the FV-MOHAM at $j = 1$, the initial approximation is taken as:

$$\tilde{X}(t)_{1,0} = 0. \tag{79}$$

The corresponding homotopy is constructed as follows:

$$\begin{aligned}\tilde{X}(t)_{1,1} &= (C_{1,1,1} + C_{1,2,1}t + C_{1,3,1}t^2)[\tilde{X}(t)_0 - r((2t(3 - 3\cos(t) - t^2))) - \int_0^t (t\cos(s-t))\tilde{X}(s)_{1,0}ds] \\ &= ((C_{1,1} + C_{1,2}t + C_{1,3}t^2)(-(r^5 + 2r)(2t(3 - 3\cos(t) - t^2))),\end{aligned} \tag{80}$$

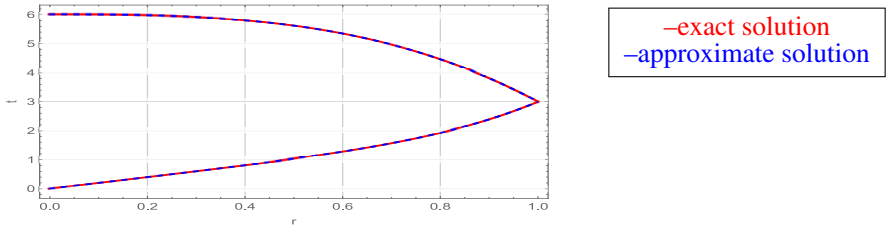

Figure 5. The approximate solutions (upper and lower) for Example 2 using fourth-order FV-OHAM at $t = 0.5$ and $r \in [0, 1]$ with the exact solution.

whereby the first approximation is

$$\tilde{H}(t)_{1,1} = \tilde{X}(t)_{1,0} + \tilde{X}(t)_{1,1} = (C_{1,1,1} + C_{1,2,1}t + C_{1,3,1}t^2)(-(r^5 + 2r)((2t(3 - 3\cos(t) - t^2))), \tag{81}$$

with residual error,

$$R_{1,1} = \tilde{X}(t)_{1,1} - (r^5 + 2r)((2t(3 - 3\cos(t) - t^2))) - \int_0^t (t\cos(s - t))\tilde{X}(s)_{1,1}ds. \tag{82}$$

By solving for the coefficients and completing the solution with the same steps for $j = 2, 3, 4, 5$, results from FV-MOHAM can be generated. The numerical solutions and their errors are tabulated in tables 14 and 15 whereas the graphs of the approximate and exact solutions are displayed in Figure 6.

Table 14. Fourth order lower FV-MOHAM solution for Example 2 at $t = 0.5$ for all $r \in [0, 1]$ and their errors.

r	$\underline{X}_{lowerMOHAM}$	$\underline{X}_{lowerMOHAM}$	$\underline{E}_r(t, r)$
0	0	0	0
0.25	-0.04380029841095035	-0.04380029841114186	7.695255×10^{-11}
0.5	-0.08760059682190069	-0.08760059682228372	1.582790×10^{-10}
0.75	-0.13140089523285105	-0.13140089523342558	2.682690×10^{-10}
1	-0.17520119364380138	-0.17520119364456743	4.604490×10^{-10}

Table 15. Fourth order upper FV-MOHAM solution for Example 2 at $t = 0.5$ for all $r \in [0, 1]$ and their errors.

r	$\overline{X}_{upperMOHAM}$	$\overline{X}_{upperMOHAM}$	$\overline{E}_r(t, r)$
0	0.75000000000000000	0.7500000000000000	0
0.25	0.7441406250000000	0.7441406259118488	3.82929×10^{-11}
0.5	0.7031250000000000	0.7031250008615894	7.65857×10^{-11}
0.75	0.5917968750000000	0.5917968757251710	1.14879×10^{-10}
1	0.37500000000000000	0.3750000004595143	1.53171×10^{-10}

Tables 16 and 17 provide a comparison between the results of the fourth-order FV-OHAM, fourth-order FV-MOHAM, and eighth-order IFBPM for Example 2. From Table 16, fourth-order FV-MOHAM remains most

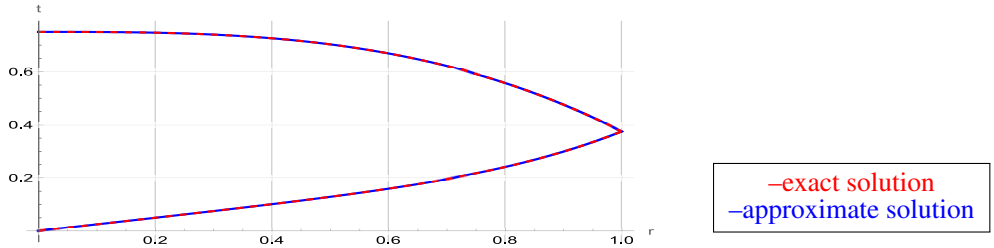

Figure 6. The approximate solutions (upper and lower) for Example 2 using the fourth-order FV-MOHAM at $t = 0.5$ and $r \in [0, 1]$ with the exact solution.

accurate in terms of the lower error compared to the other two. While both FV-OHAM and FV-MOHAM produced errors in the range of at most 10^{-9}, the higher-order IFBPM is hovering around 10^{-3} and 10^{-4}. Table 17 illustrates the same behavior in terms of the upper error. FV-OHAM exhibits satisfactory performance, with marginally greater errors than those of FV-MOHAM. Nonetheless, IFBPM continues to perform the worst in terms of the lower and upper errors. The comparison between the two tables confirm the efficacy and reliability of FV-MOHAM and FV-OHAM in reducing numerical errors, with FV-MOHAM consistently attaining the highest level of accuracy. The results underscore the efficacy of FV-MOHAM and FV-OHAM in addressing Example 2 with both lower and higher solutions, rendering them superior alternatives to IFBPM in terms of accuracy.

Table 16. Lower errors of results from the fourth-order FV-OHAM, fourth-order FV-MOHAM, and eighth-order IFBPM for Example 2 at $t = 0.5$ for $r \in [0, 1]$.

r	$FV-OHAM_{\underline{E}r(t,r)}$	$FV-MOHAM_{\underline{E}r(t,r)}$	$IFBPM_{\underline{E}r(t,r)}$ [28]
0.25	2.15841×10^{-9}	7.695255×10^{-11}	4.27470×10^{-4}
0.5	4.31682×10^{-9}	1.582790×10^{-10}	8.79930×10^{-4}
0.75	6.47522×10^{-9}	2.682690×10^{-10}	1.48240×10^{-3}
1	8.63363×10^{-9}	4.604490×10^{-10}	2.55980×10^{-3}

Table 17. Upper errors of results from the fourth-order FV-OHAM, fourth-order FV-MOHAM, and eighth-order IFBPM for Example 2 at $t = 0.5$ for $r \in [0, 1]$.

r	$FV-OHAM_{\overline{E}_r(t,r)}$	$FV-MOHAM_{\overline{E}_r(t,r)}$	$IFBPM_{\overline{E}r(t,r)}$ [28]
0.25	2.15841×10^{-9}	0	5.0769×10^{-3}
0.5	4.31682×10^{-9}	3.82929×10^{-11}	4.7996×10^{-3}
0.75	6.47522×10^{-9}	7.65857×10^{-11}	4.0397×10^{-3}
1	8.63363×10^{-9}	1.14879×10^{-10}	2.5598×10^{-3}

9. Conclusion

This research presents FV-OHAM and FV-MOHAM as novel analytical approximation techniques specifically developed to address FIEs. These approaches exhibit enhanced performance by delivering solutions as polynomial functions, accurately encapsulating the convergence of the series solution. A case study on VFIEs substantiates

the effectiveness of FV-OHAM and FV-MOHAM, underpinned by a convergence analysis. Furthermore, a second-order linear VFIE test problem is addressed to further demonstrate the correctness and efficacy of the proposed methods. The numerical findings demonstrate that both FV-OHAM and FV-MOHAM surpass HAM, Taylor method, VIM, and IFBPM in terms of accuracy and computing economy. FV-MOHAM routinely surpasses FV-OHAM, exhibiting enhanced accuracy and stability. The adaptability of these methods renders them suitable for several domains, including physics and engineering, where precision and dependability are crucial. Due to its robust performance, FV-MOHAM is especially adept at tackling real-world engineering challenges, while both approaches exhibit potential for solving higher-dimensional and more intricate problems, Future research directions could extend these methods to nonlinear FIEs, and systems of second and nth-order FVIEs.

REFERENCES

1. Kress, R. , *Linear integral equations*, Vol. 33, No. 4, Winter (1999).
2. Zwillinger, D., & Corduneanu, C., *Handbook of Differential Equations*, (1991).
3. Delves, L. M., & Mohamed, J.; Baker, C. T. H. (1977).
4. Stakgold, I., & Holst, M.; Gripenberg, G., et al. (1990).
5. Özişik, M. N.; Modest, M. F. (2013).
6. Schleicher, J., Tygel, M., & Hubral, P., An integral equation method for seismic modelling and inversion, Mathematical Methods in Geophysics, 123, 187–217 (1993).
7. Anakira, N.R., Almalki, A., Katatbeh, D., Hani, G.B., Jameel, A.F., Al Kalbani, K.S., & Abu-Dawas, M., An Algorithm for Solving Linear and Non-Linear Volterra Integro-Differential Equations, International Journal of Advances in Soft Computing & Its Applications, 15(3), (2023).
8. Gripenberg, G., Londen, S.-O., & Staffans, O., Volterra Integral and Functional Equations, Cambridge University Press, (1990).
9. Friedman, M., Ma, M., & Kandel, A., On Fuzzy Integral Equations, Fundamenta Informaticae, 37(1-2), 89–99 (1999).
10. Xu, Y., & Guo, M., A class of fuzzy integral equations with Volterra and Fredholm integral operators, Journal of Fuzzy Mathematics, 12(4), 651–667 (2004).
11. Ibrahim, R., Esa, R. H., & Jameel, A. F., Numerical treatment for solving fuzzy Volterra integral equations by sixth-order Runge-Kutta method, Mathematics and Statistics, 9(2), 123–134 (2021).
12. Gomes, L. T., Carvalho de Barros, L., & Bede, B., Fuzzy Differential Equations, Springer Briefs in Mathematics, (2015).
13. Bica, A. M., Iterative numerical method for nonlinear fuzzy Volterra integral equations, Journal of Intelligent & Fuzzy Systems, 32(3), 1639–1648 (2017).
14. Ezzati, R., Iterative fuzzy Bernstein polynomials method for nonlinear fuzzy Volterra integral equations, Computational & Applied Mathematics, 39(5), 137–150 (2020).
15. Hmaidi, J. T. A., Analytical and numerical solutions of second-kind linear fuzzy Volterra integral equations, Master's Thesis, An-Najah National University, (2016).
16. Al-Hayani, W., & Al-Bayati, Y. A., The Homotopy Analysis Method to solve the nonlinear system of Volterra integral equations and applying the genetic algorithm to enhance the solutions, European Journal of Pure and Applied Mathematics, 16(2), 345–356 (2023).
17. Jameel, A. F., Anakira, N. R., Alomari, A. K., Man, N. H., Solution and analysis of fuzzy Volterra integral equations via homotopy analysis method, Computer Modeling in Engineering Sciences, 136(1), 45–62 (2021).
18. Kutsal, S., Elastic stress analysis of hyperbolic rotating disks via optimal homotopy asymptotic method, International Journal of Engineering Research in Mechanical and Civil Engineering, 12(4), 145–155 (2023).
19. Ene, R. D., & Pop, N., Optimal Homotopy Asymptotic Method for an Anharmonic Oscillator: Application to the Chen System, Mathematics, 11(3), 210–220 (2023).
20. Jan, H. U., Ullah, H., Fiza, M., Khan, I., Mohamed, A., & Mousa, A., Modification of optimal homotopy asymptotic method for a multi-dimensional time-fractional model of Navier–Stokes equation, Fractals, 31(6), 124–134 (2023).
21. Anakira, N.R., Alomari, A.K., Jameel, A.F., and Hashim, I., Multistage optimal homotopy asymptotic method for solving initial-value problems, Journal of Nonlinear Sciences and Applications, 9(04), pp.1826–1843 (2016).
22. Zadeh, L. A., Fuzzy Sets, Information and Control, 8(3), 338–353 (1965).
23. Dubois, D., & Prade, H., Fuzzy Sets and Systems: Theory and Applications, Academic Press, (1980).
24. Jaharuddin. (2015). Optimal homotopy asymptotic method for solving Gardner equation. Applied Mathematical Sciences, 9(53), 2635–2644.
25. Aswad, N., Rahman, A., & Ahmad, M. Z. (2017). Solving fuzzy Volterra integral equations via fuzzy Sumudu transform. Applied Mathematics and Computational Intelligence, 6, 19–28.
26. Biazar, J., & Safaei, S. (2020). Applications of OHAM and MOHAM for time-fractional Klein-Fock-Gordon equation. International Journal of Optical Photonic Engineering, 5, 026.
27. Awwad, M. S., & Ababneh, O. Y. (2016). Application of optimal homotopy asymptotic method for solving linear boundary value problems differential equation. General Letters in Mathematics, 1(3), 81–94.
28. Khaji, R., Yaseen, F., & Khalil, R. I. (2024). Solution of fuzzy Volterra integral equations using composite method. Advanced Mathematical Models & Applications, 9(1), 93–104.
29. O. Kaleva, Fuzzy differential equations, Fuzzy Sets Systems, 24 (1987) 301-317.
30. Park, J. Y., Han, H. K. (1999). Existence and uniqueness theorem for a solution of fuzzy Volterra integral equations. Fuzzy Sets System, 105(3), 481–488. DOI 10.1016/S0165-0114(97)00238-8.

31. Jameel, A. F., Ismail, A. I. M., & Mabood, F. (2016). Optimal homotopy asymptotic method for solving nth-order linear fuzzy initial value problems. Journal of the Association of Arab Universities for Basic and Applied Sciences, 21, 77–85.
32. Jameel, A. F., Saaban, A., Altaie, S. A., Anakira, N. R., Alomari, A. K., & Ahmad, N. (2018). Solving first-order nonlinear fuzzy differential equations using optimal homotopy asymptotic method. International Journal of Pure and Applied Mathematics, 118(1), 49–64.
33. Jameel, A. F., Anakira, N. R., Alomari, A. K., Man, N. H. (2021). Solution and analysis of fuzzy Volterra integral equations via homotopy analysis method. Computer Modeling in Engineering Sciences, 136(1), 45–62. DOI: 10.32604/cmes.2021.014460.
34. Ziari, S., Bica, A. M., & Ezzati, R. (2020). Iterative fuzzy Bernstein polynomials method for nonlinear fuzzy Volterra integral equations. Computational and Applied Mathematics, 39(1), 316.